

Intratumoral Spatial Heterogeneity at Perfusion MR Imaging Predicts Recurrence-free Survival in Locally Advanced Breast Cancer Treated with Neoadjuvant Chemotherapy



Jia Wu, PhD • Guohong Cao, MD • Xiaoli Sun, MD • Juheon Lee, PhD • Daniel L. Rubin, MD, MS • Sandy Napel, PhD • Allison W. Kurian, MD, MSc • Bruce L. Daniel, MD • Ruijiang Li, PhD

From the Departments of Radiation Oncology (J.W., J.L., R.L.), Radiology (D.L.R., S.N., B.L.D.), Biomedical Data Science and Medicine (Biomedical Informatics Research) (D.L.R.), Medicine (A.W.K.), and Health Research and Policy (A.W.K.) and the Stanford Cancer Institute (A.W.K., R.L.), Stanford University School of Medicine, 1070 Arastradero Rd, Palo Alto, CA 94304; Department of Radiology, International Hospital of Zhejiang University, Hangzhou, Zhejiang, China (G.C.); and Department of Radiation Therapy, the First Affiliated Hospital of Zhejiang University, Hangzhou, Zhejiang, China (X.S.). Received October 20, 2017; revision requested December 6; revision received January 11, 2018; final version accepted January 12. **Address correspondence to** R.L. (e-mail: rli2@stanford.edu).

Supported by the National Cancer Institute (grants R01 CA193730, R01 CA222512, K99 CA218667).

Conflicts of interest are listed at the end of this article.

See also the editorial by Gillies and Balagurunathan in this issue.

Radiology 2018; 288:26–35 • <https://doi.org/10.1148/radiol.2018172462> • Content codes:  

Purpose: To characterize intratumoral spatial heterogeneity at perfusion magnetic resonance (MR) imaging and investigate intratumoral heterogeneity as a predictor of recurrence-free survival (RFS) in breast cancer.

Materials and Methods: In this retrospective study, a discovery cohort ($n = 60$) and a multicenter validation cohort ($n = 186$) were analyzed. Each tumor was divided into multiple spatially segregated, phenotypically consistent subregions on the basis of perfusion MR imaging parameters. The authors first defined a multiregional spatial interaction (MSI) matrix and then, based on this matrix, calculated 22 image features. A network strategy was used to integrate all image features and classify patients into different risk groups. The prognostic value of imaging-based stratification was evaluated in relation to clinical-pathologic factors with multivariable Cox regression.

Results: Three intratumoral subregions with high, intermediate, and low MR perfusion were identified and showed high consistency between the two cohorts. Patients in both cohorts were stratified according to network analysis of multiregional image features regarding RFS (log-rank test, $P = .002$ for both). Aggressive tumors were associated with a larger volume of the poorly perfused subregion as well as interaction between poorly and moderately perfused subregions and surrounding parenchyma. At multivariable analysis, the proposed MSI-based marker was independently associated with RFS (hazard ratio: 3.42; 95% confidence interval: 1.55, 7.57; $P = .002$) adjusting for age, estrogen receptor (ER) status, progesterone receptor status, human epidermal growth factor receptor type 2 (HER2) status, tumor volume, and pathologic complete response (pCR). Furthermore, imaging helped stratify patients for RFS within the ER-positive and HER2-positive subgroups (log-rank test, $P = .007$ and $.004$) and among patients without pCR after neoadjuvant chemotherapy (log-rank test, $P = .003$).

Conclusion: Breast cancer consists of multiple spatially distinct subregions. Imaging heterogeneity is an independent prognostic factor beyond traditional risk predictors.

© RSNA, 2018

Online supplemental material is available for this article.

Neoadjuvant chemotherapy is used to treat locally advanced breast cancer with the goal of downstaging tumors and increasing breast conservation rates (1). Pathologic complete response (pCR) after neoadjuvant chemotherapy has been demonstrated to be a favorable prognostic marker in terms of recurrence-free survival (RFS) in the Investigation of Serial Studies to Predict Your Therapeutic Response with Imaging and Molecular Analysis (I-SPY 1 TRIAL) (2). Tumor burden as measured with functional tumor volume at magnetic resonance (MR) imaging early during neoadjuvant chemotherapy has also been shown to be associated with RFS in the I-SPY 1 TRIAL (3). Yet, the accuracy of predicting recurrence on an individualized basis is still limited (4), as breast cancer is known to be a heterogeneous disease with

wide variations in outcomes and response to therapy. The identification of additional prognostic markers beyond current factors such as pCR and tumor volume would allow more refined patient stratification and potentially guide risk-adaptive personalized therapy (5).

Radiomics investigates a large number of computational image features and is a promising approach for identifying imaging markers (6–8). Some radiomic features, such as tumor texture, may be useful for differentiating malignant from benign tumors or for evaluating treatment response and outcome in breast cancer (9–16). Although texture features provide a measure of intratumoral heterogeneity to a certain extent, this characterization is incomplete because their calculation applies to the whole tumor. As such, this approach assumes that

Abbreviations

DCE = dynamic contrast material enhanced, ER = estrogen receptor, HER2 = human epidermal growth factor receptor type 2, I-SPY 1 TRIAL = Investigation of Serial Studies to Predict Your Therapeutic Response with Imaging and Molecular Analysis, MSI = multiregional spatial interaction, pCR = pathologic complete response, PR = progesterone receptor, RFS = recurrence-free survival

Summary

We discovered and validated three intratumoral subregions with distinct MR perfusion imaging parameters. In addition to clinical-pathologic and genomic factors, intratumoral spatial heterogeneity characterized by MR imaging was an independent predictor of recurrence-free survival in two breast cancer cohorts.

Implications for Patient Care

- Intratumoral spatial heterogeneity at MR imaging delivers additional prognostic value beyond current clinical-pathologic and biologic predictors in breast cancer, providing a proposed imaging marker for future therapy.
- Intratumoral spatial heterogeneity at MR imaging could potentially be used to stratify patients for risk-adaptive individualized therapy.
- The proposed methodology to define and characterize intratumoral spatial heterogeneity will be applicable to other cancer types.

the tumor is heterogeneous but well mixed, thus neglecting regional phenotypic variations within a tumor (17).

In our study, we aimed to discover intrinsic intratumoral subregions of breast cancer defined by multiparametric perfusion imaging maps and to investigate the reproducibility of these discovered subregions in another independent cohort. We used multiregional image features to characterize intratumoral spatial heterogeneity and investigate their association with RFS to determine whether imaging heterogeneity provides independent prognostic value beyond existing risk predictors.

Materials and Methods

Overview of Study Design and Patient Cohorts

This retrospective study was approved by the institutional review board and compliant with the Health Insurance Portability and Accountability Act. Our study was carried out in three steps, as shown in Figure E1 (online). First, we discovered spatially distinct intratumoral subregions of breast cancer on the basis of perfusion imaging parameters and validated their consistency in two independent cohorts. Second, we characterized spatial heterogeneity by quantifying multiregional interactions from intratumoral subregion maps and evaluated their reproducibility against uncertainty in tumor delineation. Third, we developed a network strategy to stratify patients into different groups on the basis of image features and assessed its clinical relevance in relation to clinical-pathologic and genomic factors for predicting RFS.

Two breast cohorts were analyzed, including 60 patients treated at the University of California, San Francisco, between 1995 and 2002 for discovery purposes (cohort 1) and 186 patients from the I-SPY 1 TRIAL treated between 2002 and 2006 (2) for validation purposes (cohort 2). Patient characteristics of

these two cohorts are summarized in Table 1. Details of patient cohorts and imaging protocols are shown in Figure 1 and Appendix E1 (online).

Discovery and Validation of Intratumoral Subregions

After image harmonization and tumor delineation (details in Appendix E1 [online]), we developed a robust intratumor partitioning method to divide the tumor into multiple spatially segregated, phenotypically consistent subregions. As outlined in Figure 2a, this method consists of a two-stage clustering process. First, at the individual level, each tumor is oversegmented into many small contiguous regions (ie, superpixels) that contain similar voxels as defined by four kinetic maps at dynamic contrast material-enhanced (DCE) MR imaging: percentage enhancement, signal enhancement ratio, and wash-in and washout slopes (9,18,19), as detailed in Appendix E1 (online) and Figure E2 (online). Second, at the population level, all superpixels from the entire population are aggregated and consistently labeled by means of consensus cluster (Appendix E1 [online]), where similar superpixels within the same tumor are merged to form a subregion. In this way, the correspondence between tumor subregions can be established across patients in a given population.

We independently applied the proposed tumor partitioning method in two breast cancer cohorts (cohorts 1 and 2) to validate the consistency of the defined intratumoral subregions via the in-group proportion statistic (20), as detailed in Appendix E1 (online). We used the significance analysis of microarrays algorithm (21) to identify perfusion imaging parameters that are associated with the revealed subregions in both cohorts.

Quantitative Image Features to Characterize Intratumoral Spatial Heterogeneity

On the basis of the discovered multiregion maps, we used the multiregional spatial interaction (MSI) matrix to characterize and quantify the intratumoral spatial heterogeneity. In detail, the neighbor of every tumor voxel was probed, where the resulting pair was added to the appropriate entry in the MSI matrix, as shown in Figure 2b. This process was repeated until all tumor voxels were iterated, and the spatial heterogeneity was summarized in the final MSI matrix. Of note, we included the breast parenchyma as one distinct region to explicitly account for the spatial relationship between the tumor subregions and its surrounding tissue. Intuitively, the diagonal elements of the MSI matrix represent connected size for individual subregions, whereas the off-diagonal elements relate to the size of borders where different subregions meet. A total of 22 features were extracted from the MSI matrix, including 18 first-order and four second-order statistical features as explained in Figure 2c. Together, they quantify the degree and spectrum of intratumoral spatial heterogeneity revealed by multiregional maps.

Network Analysis to Stratify Patients into Distinct Clusters

We developed a network-based strategy to explore the similarity between patients and to discover patterns of breast can-

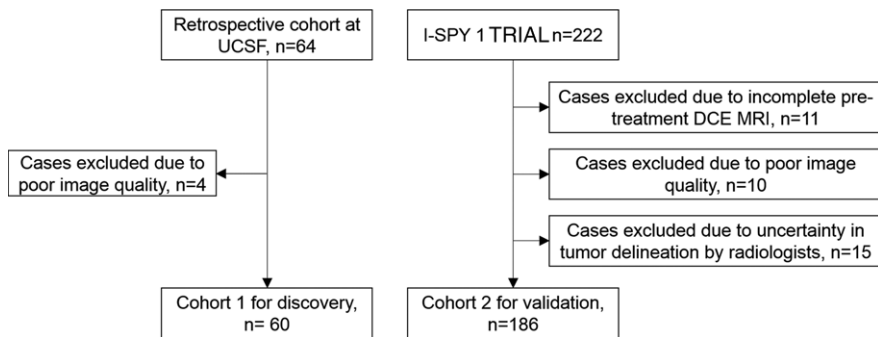


Figure 1: Flowchart shows number of patients with breast cancer in two study cohorts. DCE = dynamic contrast-enhanced, I-SPY 1 TRIAL = Investigation of Serial Studies to Predict Your Therapeutic Response with Imaging and Molecular Analysis, UCSF = University of California, San Francisco.

cer heterogeneity in a single-institution cohort (cohort 1). In detail, a fully connected graph was built to model the pairwise relations between patients based on the aforementioned 22 image features (Fig 2c). The vertices correspond to individual patients and the edges were weighted by the similarity between connected patients. The similarity was measured with Euclidean distance in the space formed by 22 image features and further smoothed by the radial basis kernel. Next, the patient similarity graph was analyzed with the spectral clustering method (22) to divide patients into distinct clusters. Compared with traditional unsupervised clustering algorithms, spectral clustering is known to be a robust method for discovering nonconvex and linearly nonseparable clusters (22), which is ideally suitable for handling heterogeneous breast cancer data in our study. Given network-based patient stratification in the discovery cohort, we propagated the patient cluster labels to the validation cohort (cohort 2) by using a robust label propagation algorithm (23), as detailed in Appendix E1 (online). No information about prognosis in cohort 2 was used during the propagation procedure to ensure further independent validation.

Clinical Relevance of Network-based Patient Stratification with Imaging and Multivariable Analysis Adjusting for Existing Risk Factors

We evaluated the imaging-based patient stratification in terms of its prognostic capacity for predicting RFS in the discovery cohort and then tested it in the independent I-SPY 1 TRIAL cohort. We investigated the relationships between the proposed imaging marker and existing clinical-pathologic and genomic predictors of RFS and tested whether it provided independent prognostic value by using multivariable Cox regression analysis. According to the latest National Comprehensive Cancer Network guidelines of invasive breast cancer (24), risk factors include age, estrogen receptor (ER) status, progesterone receptor (PR) status, human epidermal growth factor receptor type 2 (HER2) status, stage, pathologic grade, and lymph node metastasis. In addition, pCR was shown to be a strong predictor of RFS in the I-SPY 1 TRIAL cohort (2) and therefore was included in our analysis. Keeping significant covariates, we further adjusted them for the 70-gene MammaPrint

microarray assay (Agendia, Amsterdam, the Netherlands) recurrence score and the 50-gene PAM50 assay (Nanostring Technologies, Seattle, Wash) subtypes in a subset of I-SPY 1 TRIAL patients ($n = 128$) with available microarray data in Gene Expression Omnibus (<https://www.ncbi.nlm.nih.gov/geo/>, tracking number GSE22226). Next, we performed subgroup analysis to determine whether the proposed imaging marker can enable further stratification of patients within certain clinically meaningful subgroups. Finally, we compared our imaging marker with conventional whole-tumor texture features based on

the gray-level co-occurrence matrix that have been widely used to measure tumor heterogeneity (25,26) as well as simple perfusion parameters derived from the intratumoral subregions.

Evaluation of Reproducibility with Respect to Variation in Tumor Segmentation

Our proposed computational pipeline is fully automatic once the tumor contour is delineated by radiologists. Given the uncertainty in tumor delineation, we investigated the reproducibility of our results at various stages with respect to tumor contours (details in Appendix E1 [online]).

Statistical Analysis

We fit the Cox proportional hazard model between different risk predictors and RFS. Kaplan-Meier analysis and the log-rank test were used to evaluate patient stratification into different risk groups. The hazard ratio was used to measure the degree of survival differences. For the I-SPY 1 TRIAL cohort, we censored the patients alive at 5 years to alleviate confounding effects by comorbidities, as was done in the primary publication (2). All statistical tests were two-sided, with $P < .05$ indicative of a statistically significant difference. All statistical analyses were performed in R (R Foundation for Statistical Computing, Vienna, Austria).

Results

Identification and Validation of Three Intratumoral Subregions

Patients from the two cohorts had similar distribution for ER, PR, and HER2 status, and the median follow-up time was 6.67 years for cohort 1 and 4.12 years for cohort 2 (Table 1). We independently applied our proposed tumor partitioning method in cohorts 1 and 2 and determined the optimal number of intratumoral subregions. As shown in Figures E3, A (online), and E4, A (online), there are three distinct clusters (ie, subregions) in each cohort according to hierarchical clustering on consensus matrix. This was further confirmed by cumulative distribution function curves in Figures E3, B and C (online), and E4, B and C (online). The three intratumoral subregions were highly consistent

across the two cohorts, with corresponding in-group proportion values of 97.8%, 99.0%, and 98.6%, respectively, for subregions 1, 2, and 3 ($P < .001$).

We then investigated what imaging parameters are associated with the three intratumoral subregions and how they can be differentiated with kinetic features. Figure 3 shows the detailed distributions of the four perfusion parameters (signal enhancement ratio, percentage enhancement, wash-in slope, and washout slope) in each of three subregions. The sorted perfusion maps derived from DCE MR imaging associated with each subregion in two cohorts are shown in Figure E5 (online). From these results, we observed a consistent pattern in both cohorts where the four perfusion parameters all increased from subregion 1 to 3. We thus concluded that subregions 1, 2, and 3 represent poorly, moderately, and highly perfused subregions in the tumor, respectively.

Network-based Patient Stratification according to Imaging Heterogeneity in Two Independent Cohorts

Once the intratumoral subregions were identified, we extracted 22 image features to characterize tumor spatial heterogeneity and applied network analysis to stratify patients in the discovery cohort. Figure 4, A, shows the topological relationship of the patients in a sparse graph to facilitate visualization. We used a spectral clustering algorithm to divide patients into two groups, showing significant differences in RFS (log-rank test, $P = .002$) (Fig 4, B).

To test the prognostic value of imaging heterogeneity in an independent cohort, we first trained a multinomial model based on four perfusion parameters to classify each voxel into one of the three subregions. The details of this model, which had an overall accuracy of 0.975, are shown in Table E1 (online). Then, we applied this model to define intratumoral subregions in the validation cohort (cohort 2). The same 22 image features were extracted to characterize spatial heterogeneity. Finally, given the clustering results in the discovery cohort, we separated patients in the

Table 1: Summary of Demographic and Clinical Data from the Two Study Cohorts

Parameter	Discovery Set: Cohort 1 ($n = 60$)	Validation Set: Cohort 2 ($n = 186$)
Age (y)		
Median*	48.1 (29.7–72.4)	49.1 (26.7–68.8)
Mean \pm standard deviation	48.0 \pm 9.9	48.4 \pm 9.1
Estrogen receptor		
Positive	28 (47)	103 (55)
Negative	20 (33)	82 (44)
Unknown	12 (20)	1 (1)
Progesterone receptor		
Positive	22 (37)	87 (47)
Negative	26 (43)	98 (53)
Unknown	12 (20)	1 (1)
Human epidermal growth factor receptor type 2		
Positive	14 (23)	56 (30)
Negative	31 (52)	126 (68)
Unknown	15 (25)	4 (2)
Histologic type		
Invasive ductal carcinoma	37 (62)	...
Invasive lobular carcinoma	11 (18)	...
Other	12 (20)	...
Pathologic grade		
1	...	10 (5)
2	...	57 (31)
3	...	60 (32)
Unknown	...	59 (32)
Lymph node metastasis		
Yes	36 (60)	...
No	23 (38)	...
Unknown	1 (2)	...
Follow-up (y) [†]		
Median*	6.67 (0.95–9.84)	4.12 (0.51–6.9)
Mean \pm standard deviation	6.05 \pm 2.35	4.13 \pm 1.21
Recurrence		
Yes	22 (37)	51 (27)
No	37 (62)	135 (73)
Unknown	1 (2)	0
Pathologic complete response		
Yes	...	50 (27)
No	...	131 (70)
Unknown	...	5 (3)
Transcriptional data		
Available	...	128 (69)
Missing	...	58 (31)

Note.—Unless otherwise indicated, data are numbers of patients, with percentages in parentheses.

* Numbers in parentheses are the range.

[†] Computed with subjects without recurrence.

validation cohort into low- and high-risk groups by using a robust label propagation algorithm. Consistent with the discovery cohort, a significant difference in RFS was observed between the two groups in the validation cohort (log-rank test, $P = .002$) (Fig 5, A).

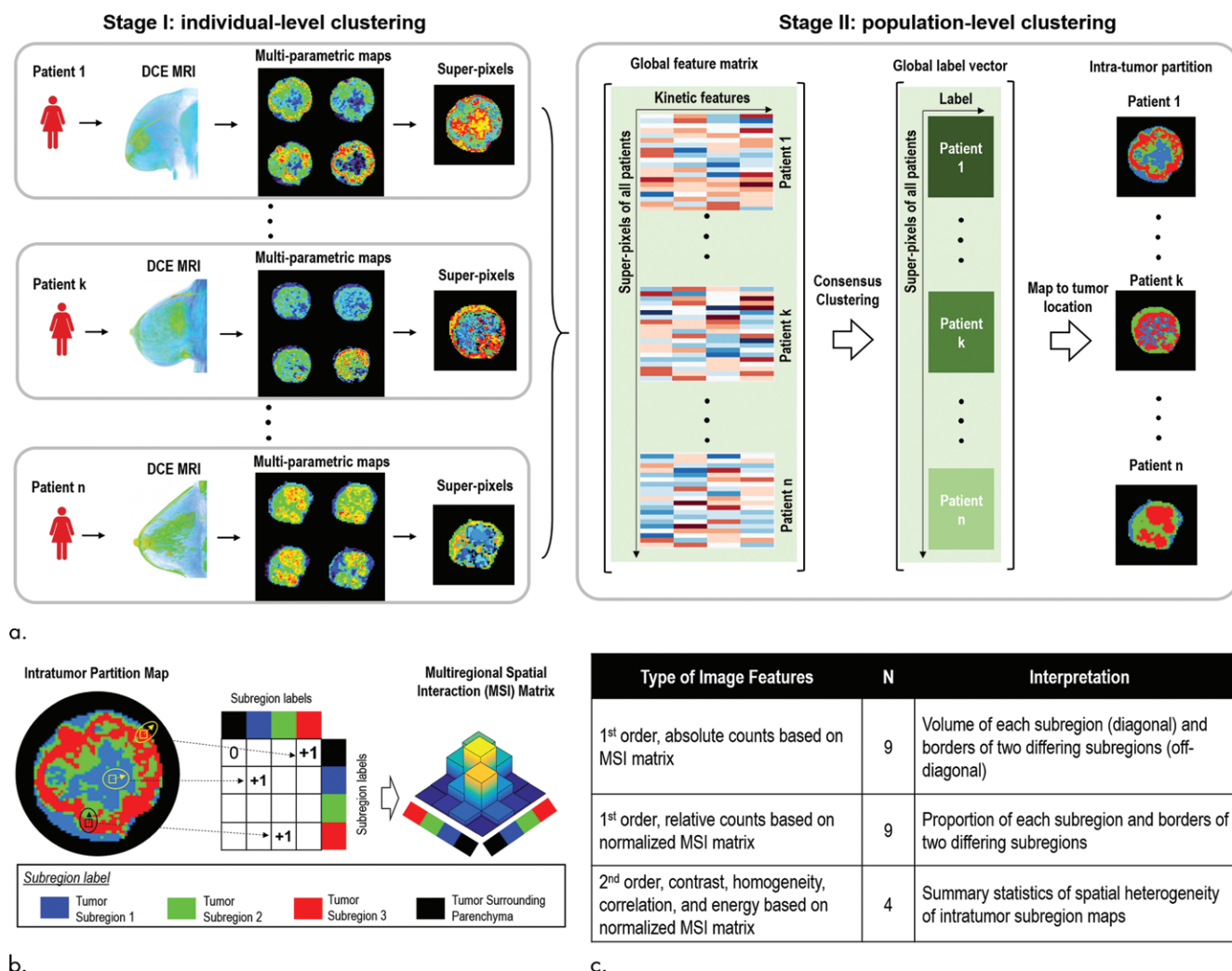


Figure 2: (a) Proposed two-stage intratumor partition framework. DCE = dynamic contrast-enhanced. (b) Illustration shows use of multiregional spatial interaction (MSI) matrix derived from intratumor partition maps. (c) Twenty-two quantitative imaging features were extracted from MSI matrix to measure intratumoral spatial heterogeneity.

Multiregional Imaging Phenotypes Are Associated with Aggressive Disease and Poor Prognosis and Outperform Whole Tumor-based Texture Analysis

On the basis of significance analysis of microarrays, several image features were differentially expressed between the low- and high-risk groups in terms of RFS (Table E2 [online]). In particular, tumors in the high-risk patient group were characterized by larger volume of the poorly perfused intratumoral subregion, larger volume of interaction between poorly and moderately perfused subregions and surrounding parenchyma, and higher homogeneity and correlation of the MSI matrix. Figure 6 shows the detailed intratumor partition maps of two representative patients with similar clinical-pathologic factors, where the proposed pipeline correctly predicted their recurrence risk. These patterns were consistent in both discovery and validation cohorts (Table E2 [online]). In comparison, none of the whole tumor-based morphologic or texture features were prognostic of RFS; moreover, the simple kinetic measures of intratumoral subregions were not consistent predictors of RFS in both cohorts (Fig E6 [online]).

Independent Prognostic Value of Imaging beyond Traditional Risk Predictors

In multivariable analysis of the discovery cohort, our proposed imaging heterogeneity-based patient stratification was the only variable associated with RFS ($P = .022$) after adjusting for clinical-pathologic factors such as age, ER status, PR status, HER2 status, histologic type, and lymph node metastasis (Table E3 [online]). Importantly, this result was validated in the I-SPY 1 TRIAL cohort, where our imaging marker showed independent prognostic value when adjusting for age, ER status, PR status, HER2 status, tumor volume, and pCR (Table 2). We further adjusted with pathologic grade, PAM50 subtype, and MammaPrint score for a subset of patients in the I-SPY 1 TRIAL cohort ($n = 121$) with available information through Gene Expression Omnibus (tracking number GSE22226). The proposed imaging marker remained as an independent predictor of RFS ($P = .022$) (Table E4 [online]).

In subgroup analysis, our proposed imaging marker further stratified patients for RFS within ER-positive and HER2-

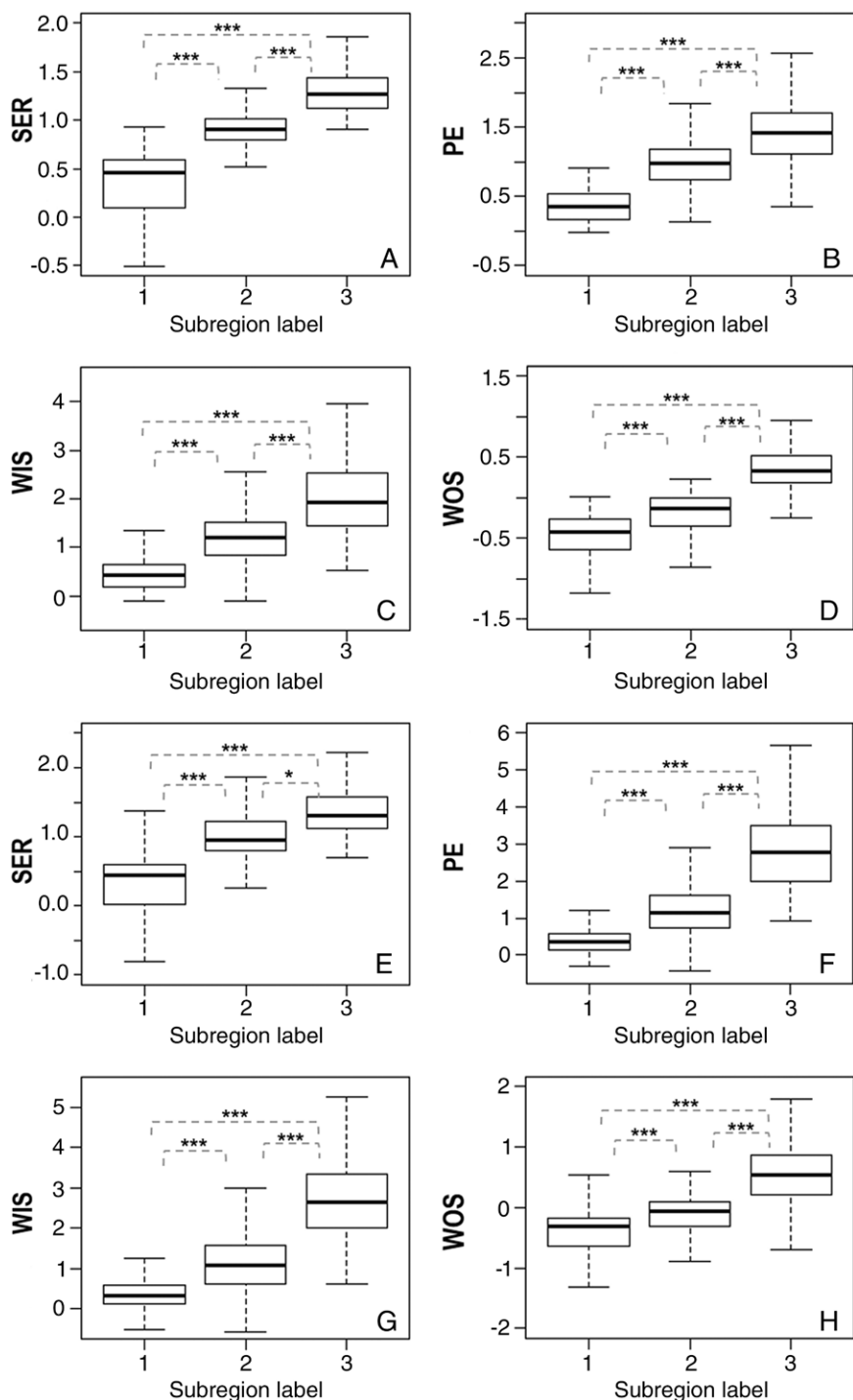


Figure 3: Box-and-whisker plots show distribution of four perfusion imaging parameters for three intratumoral subregions for, A–D, cohort 1 and, E–H, cohort 2. PE = percentage enhancement, SER = signal enhancement ratio, WIS = wash-in slope, WOS = washout slope. P values were obtained with Student *t* test. * = $P < .05$, ** = $P < .001$, *** = $P < .0001$.

positive breast cancer (log-rank test, $P = .007$ and $.004$, respectively) (Fig 5, B, C) but did not show an association for the ER-negative, PR-negative, HER2-negative, or triple-negative subgroups (Fig E7, A [online]). For patients without pCR ($n = 131$), our imaging marker was strongly prognostic of RFS (log-rank test, $P = .003$) (Fig 5, D). For the pCR

subgroup, we observed a similar trend but no association, likely due to the small sample size (Fig E7, B [online]).

High Reproducibility between Manual and Automated Tumor Segmentation

A high correlation existed for manual and automated tumor contours, with $R^2 = 0.98$ and an average Dice coefficient of 0.87 (Fig E8 [online]). With automated tumor contours, the partitioning procedures identified three intratumoral subregions with similar perfusion characteristics (Figs E9, E10 [online]). There was good agreement between the original and recalculated MSI-based features, with a mean intraclass correlation coefficient of 0.85 (Fig E11, A [online]). Compared with the original stratification, the predicted cluster labels of only four patients were inconsistent, as shown in Figure E11, B (online). Results of the χ^2 test further confirmed the high dependency for two alternative ways of patient stratification ($P = 2.3E-10$). Furthermore, the Kaplan-Meier plot of RFS based on automated tumor contours (Fig E11, C [online]) had an excellent agreement to that based on manual contours (Fig 4, B).

Discussion

In this study, we showed that multiregional image features extracted from baseline DCE MR images can be used to characterize intratumoral spatial heterogeneity and detect aggressive disease in breast cancer. In two independent cohorts, multiregional image features stratified a network-based clustering of patients associated with RFS. Importantly, the imaging-based stratification provided additional prognostic value beyond traditional clinical-pathologic and genomic factors such as ER, PR, and HER2 status. The primary finding of the I-SPY 1 TRIAL is that pCR is an independent

prognostic factor in patients with locally advanced breast cancer treated with neoadjuvant chemotherapy (2). Herein, we showed that those patients without pCR in the I-SPY 1 TRIAL cohort could be further divided into groups with different prognoses by means of our imaging analyses, with a similar trend for those with pCR. Taken together, these data suggest that imaging-based

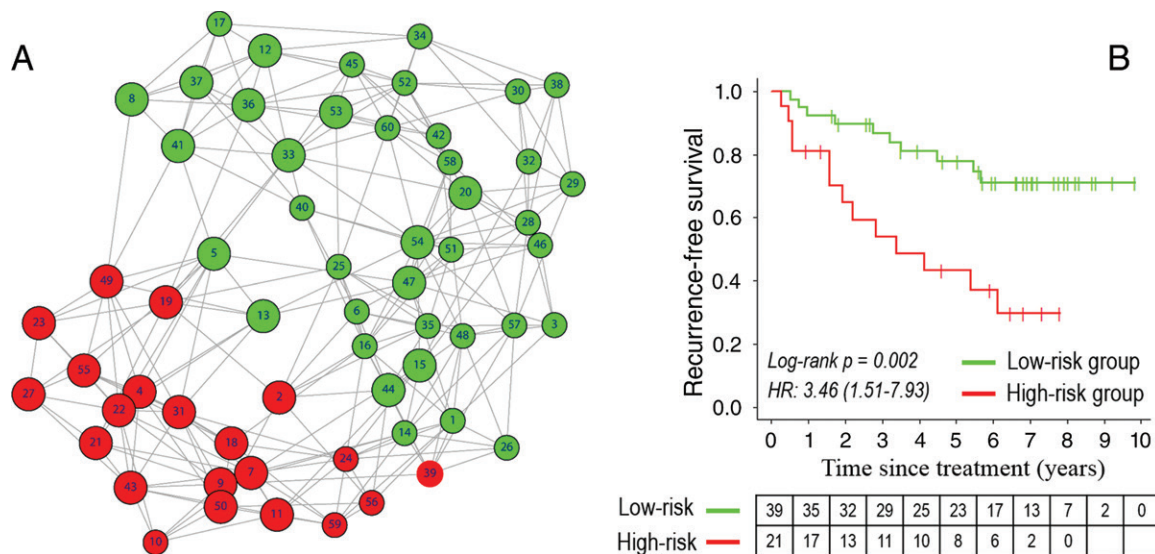


Figure 4: A, Sparse graph with seven neighbors shows 60 patients in discovery cohort after proposed network analysis. Two clusters were identified, with 21 patients in one cluster labeled in red and remaining 39 patients in another cluster labeled in green. Each vertex represents an individual patient, and its size is proportional to tumor volume. B, Kaplan-Meier curves of recurrence-free survival stratified according to the two patient clusters. Coloring is consistent with patient cluster in A.

heterogeneity can provide complementary prognostic information to existing risk predictors.

To identify prognostic imaging markers in breast cancer, Hylton et al (3) defined functional tumor volume through aggregating tumor voxels with percentage enhancement greater than 0.7, and they found that only change in this functional tumor volume from baseline to during neoadjuvant chemotherapy was associated with RFS in the I-SPY 1 TRIAL cohort, while the functional tumor volume at baseline alone was not. In our study, we discovered three intratumoral subregions with poor, moderate, and marked perfusion at DCE MR imaging and showed that spatial tumor heterogeneity characterized by multiregional image features at baseline could be used to stratify patients for RFS in two independent cohorts. Our data support that imaging heterogeneity could provide additional value to traditional volume-based imaging metrics (27).

It has been recognized that tumors demonstrate regional variations in genotypes and phenotypes owing to clonal evolution (28,29). Image-based intratumoral partitioning could reveal aggressive subregions that are important for determining prognosis and treatment response (17,30–34). In this work, we found that tumors in the high-recurrence risk group had a larger volume of the poorly perfused subregion as well as a larger volume of interaction between poorly and moderately perfused subregions and surrounding parenchyma. These imaging patterns of aggressive tumors could be driven by a hypoxic microenvironment within the tumor and at the invasive margin. Our finding is consistent with the well-established role of hypoxia in breast cancer progression, metastasis, and patient outcomes (35–37).

There are several key features that differentiate our work from previous radiomic studies. First and foremost, we explicitly account for spatial heterogeneity by dividing the tumor into multiple subregions and analyzing each subregion separately as well as their mutual relationships through a

multiregional spatial interaction matrix. In contrast, traditional studies investigate aggregate image features from the entire tumor as a whole and may not fully capture the extent of intratumoral heterogeneity. This might explain the fact that texture gray-level co-occurrence matrix-based features calculated from the whole tumor did not consistently enable prediction of RFS in our study. Another distinction from traditional radiomic studies is that they typically require feature selection and then construct a model based on selected informative features. In contrast, the proposed network stratification approach uses all relevant information to make a prediction by analyzing the pair-wise similarity pattern between patients. This approach may be less prone to the risk of overfitting as well as more robust to small training size. These technical advances contributed to the reproducible results demonstrated in our study.

One limitation of our study is the use of a particular imaging protocol for DCE MR imaging that is not universal in clinical practice. Technical factors such as field strength, repetition time, echo time, and flip angle may influence the results despite efforts to normalize imaging. Therefore, additional studies are needed to confirm and validate our findings. Another limitation is the small size of the pCR subgroup in the validation cohort. Finally, adjuvant therapies for patients in the discovery cohort were not documented, and our study largely preceded the use of trastuzumab for HER2-positive breast cancer. Whether our findings still hold in the current era of molecularly targeted therapies remains to be investigated.

In our study, we focused on clinically used diagnostic DCE MR imaging. Future work could incorporate state-of-the-art DCE MR imaging techniques with higher temporal and spatial resolution, or additional modalities such as diffusion and metabolic imaging (38–40), in defining intratumoral subregions. This might lead to the discovery of more granular imaging

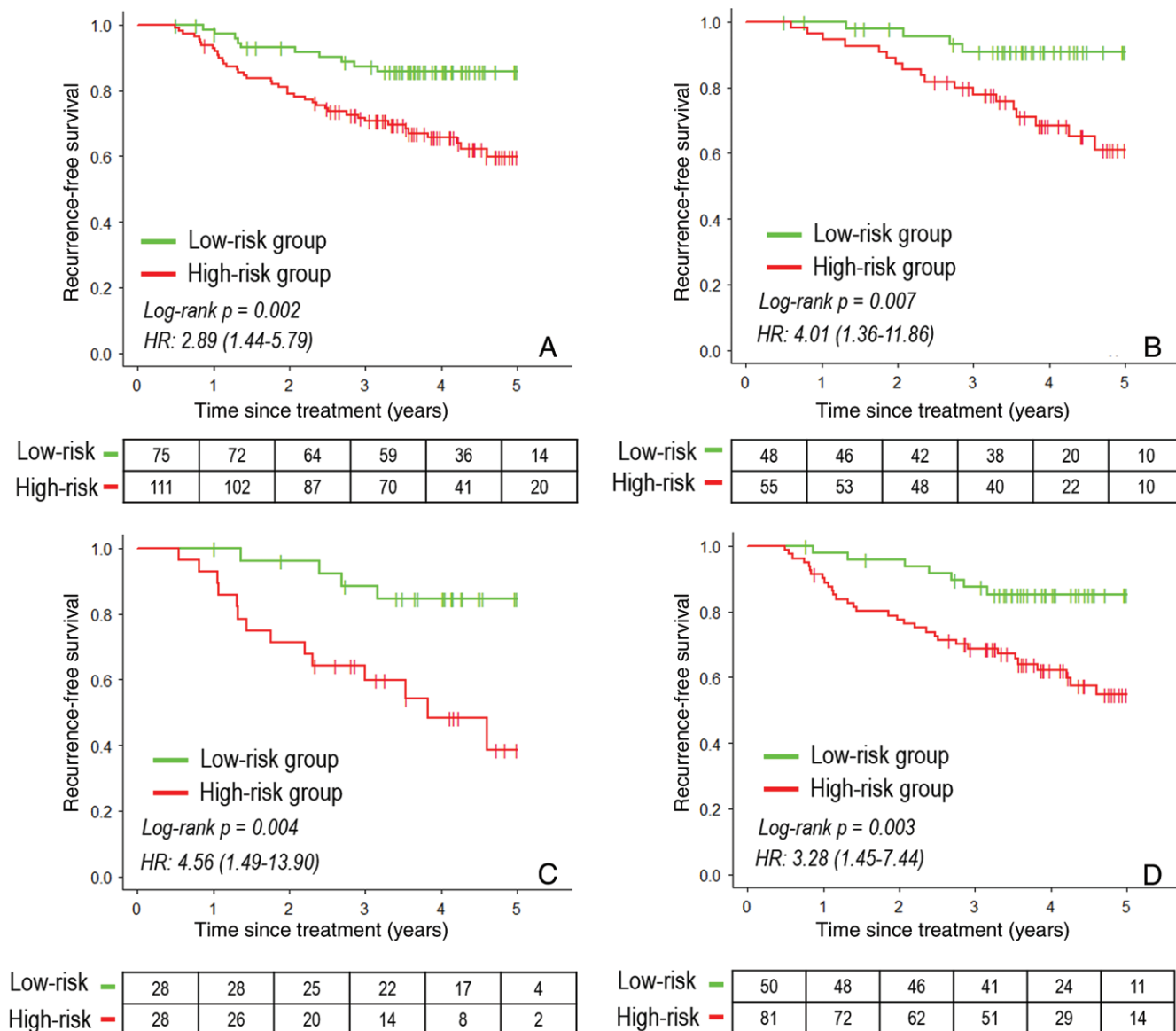


Figure 5: Kaplan-Meier curves of recurrence-free survival in validation cohort. Patients are stratified according to propagated patient cluster labels in discovery cohort (Fig 3, A). Plots are for, A, entire validation cohort (Investigation of Serial Studies to Predict Your Therapeutic Response with Imaging and Molecular Analysis), B, estrogen receptor-positive subgroup, C, human epidermal growth factor receptor type 2-positive subgroup, and, D, subgroup showing no pathologic complete response. HR = hazard ratio.

habitats and refined measurement of spatial heterogeneity. Combining intratumoral with peritumoral imaging characteristics may help improve prediction of pCR and RFS (41,42). In addition, multiple serial images (3,27,43) could help determine whether the longitudinal change of intratumoral imaging heterogeneity might better correlate with treatment response or disease progression. It may be of interest for future studies to combine imaging with pathologic or molecular data to understand the underlying biologic basis of the tumor heterogeneity captured by multiregional image features (44,45).

In summary, we discovered and validated three intratumoral subregions with distinct perfusion characteristics in breast cancer. In addition to clinical-pathologic and genomic factors, imaging heterogeneity defined by multiregional features is an

independent predictor of RFS. We envision that the proposed methodology to define and characterize intratumoral spatial heterogeneity will be applicable to other cancer types.

Acknowledgment: We thank the Cancer Imaging Archive (TCIA) for providing the breast cancer cases enrolled in the Cancer Genome Atlas (TCGA) study and the University of California, San Francisco, study.

Disclosures of Conflicts of Interest: J.W. disclosed no relevant relationships. G.C. disclosed no relevant relationships. X.S. disclosed no relevant relationships. J.L. disclosed no relevant relationships. D.L.R. disclosed no relevant relationships. S.N. Activities related to the present article: disclosed no relevant relationships. Activities not related to the present article: is on the scientific advisory board at EchoPixel, Fovia, and Radlogics; is a consultant for Carestream; has grants/grants pending with Royal Phillips; has stock/stock options in Radlogics and EchoPixel. Other relationships: disclosed no relevant relationships. A.W.K. Activities related to the present article: disclosed no relevant relationships. Activities not related to the

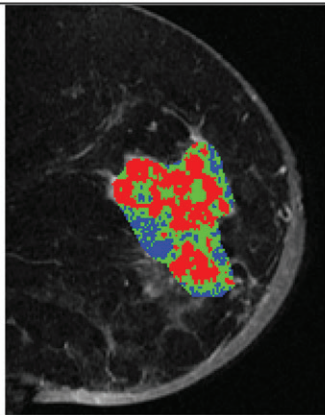
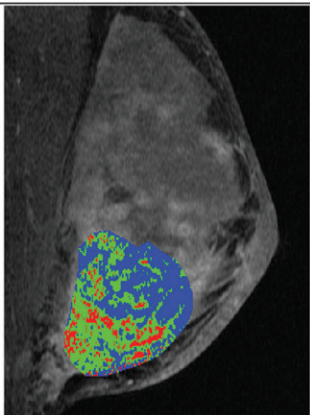
	Patient 1	Patient 2
Intratumor Partition Map		
Clinical Information	ER+, HER2-, LN+ Total tumor 40.7 cc	ER+, HER2-, LN+ Total tumor 43.1 cc
Outcome	Recurrence free at 355.7 weeks	Distant metastasis at 216 weeks
MSI Features	Burden of low perfusion 8.1 cc Low-intermedian border: 0.9 cc Low-parenchyma border: 0.3 cc	Burden of low perfusion 22.2 cc Low-intermedian border: 2.7 cc Low-parenchyma border: 1.0 cc
Prediction by Proposed Method	Low risk of recurrence	High risk of recurrence

Figure 6: Intratumor partition maps in two breast cancer patients. The proposed analysis pipeline accurately predicted their recurrence risk. High-perfusion subregion is in red, with intermediate perfusion in green and low perfusion in blue. *ER* = estrogen receptor, *HER2* = human epidermal growth factor receptor type 2, *LN* = lymph node, *MSI* = multiregional spatial interaction.

Table 2: Univariable and Multivariable Analyses of the Proposed Imaging Biomarker and Clinical Risk Factors for Predicting Recurrence-free Survival in the Validation Cohort

Predictor	Univariable Analysis			Multivariable Analysis*		
	HR	95% CI	P Value	HR	95% CI	P Value
Imaging biomarker [†]	2.89	1.44, 5.79	.003 [‡]	3.42	1.55, 7.57	.002 [‡]
Age	0.88	0.67, 1.17	.384	0.79	0.58, 1.07	.121
ER	0.59	0.34, 1.05	.072	0.44	0.18, 1.09	.075
PR	0.76	0.43, 1.36	.359	1.45	0.58, 3.63	.428
HER2	1.47	0.82, 2.65	.200	2.39	1.26, 4.51	.007 [‡]
Tumor volume	1.09	0.87, 1.37	.0456	0.99	0.74, 1.32	.942
pCR [§]	0.49	0.20, 1.00	.050 [‡]	0.34	0.15, 0.79	.012 [‡]

Note.—CI = confidence interval, ER = estrogen receptor, HER2 = human epidermal growth factor receptor type 2, HR = hazard ratio, pCR = pathologic complete response, PR = progesterone receptor.

* Nine patients were excluded because values were missing from some variables.

[†] Defined by propagation of patient labels from the discovery cohort; low-risk group was coded as 0, high-risk group as 1.

[‡] $P < .05$.

[§] Pathologic complete response was coded as 1, everything else as 0.

present article: institution has grants/grants pending with Myriad Genetics. Other relationships: disclosed no relevant relationships. **B.L.D.** disclosed no relevant relationships. **R.L.** disclosed no relevant relationships.

Author contributions: Guarantors of integrity of entire study, J.W., X.S., R.L.; study concepts/study design or data acquisition or data analysis/interpretation, all

authors; manuscript drafting or manuscript revision for important intellectual content, all authors; approval of final version of submitted manuscript, all authors; agrees to ensure any questions related to the work are appropriately resolved, all authors; literature research, J.W., J.L., A.W.K., B.L.D., R.L.; clinical studies, J.W., G.C., X.S.; statistical analysis, J.W., J.L.; and manuscript editing, J.W., G.C., D.L.R., A.W.K., B.L.D., R.L.

References

- Gralow JR, Burstein HJ, Wood W, et al. Preoperative therapy in invasive breast cancer: pathologic assessment and systemic therapy issues in operable disease. *J Clin Oncol* 2008;26(5):814–819.
- Esserman LJ, Berry DA, DeMichele A, et al. Pathologic complete response predicts recurrence-free survival more effectively by cancer subset: results from the I-SPY 1 TRIAL—CALGB 150007/150012, ACRIN 6657. *J Clin Oncol* 2012;30(26):3242–3249.
- Hylton NM, Gatsonis CA, Rosen MA, et al. Neoadjuvant chemotherapy for breast cancer: functional tumor volume by MR imaging predicts recurrence-free survival—results from the ACRIN 6657/CALGB 150007 I-SPY 1 TRIAL. *Radiology* 2016;279(1):44–55.
- Esserman LJ, Thompson IM, Reid B, et al. Addressing overdiagnosis and overtreatment in cancer: a prescription for change. *Lancet Oncol* 2014;15(6):e234–e242.
- Zardavas D, Irrthum A, Swanton C, Piccart M. Clinical management of breast cancer heterogeneity. *Nat Rev Clin Oncol* 2015;12(7):381–394.
- Aerts HJ. The potential of radiomic-based phenotyping in precision medicine: a review. *JAMA Oncol* 2016;2(12):1636–1642.
- Gillies RJ, Kinahan PE, Hricak H. Radiomics: images are more than pictures, they are data. *Radiology* 2016;278(2):563–577.
- Lambin P, Rios-Velazquez E, Leijenaar R, et al. Radiomics: extracting more information from medical images using advanced feature analysis. *Eur J Cancer* 2012;48(4):441–446.
- Bhooshan N, Giger ML, Jansen SA, Li H, Lan L, Newstead GM. Cancerous breast lesions on dynamic contrast-enhanced MR images: computerized characterization for image-based prognostic markers. *Radiology* 2010;254(3):680–690.
- Ahmed A, Gibbs P, Pickles M, Turnbull L. Texture analysis in assessment and prediction of chemotherapy response in breast cancer. *J Magn Reson Imaging* 2013;38(1):89–101.
- Parikh J, Selmi M, Charles-Edwards G, et al. Changes in primary breast cancer heterogeneity may augment midtreatment MR imaging assessment of response to neoadjuvant chemotherapy. *Radiology* 2014;272(1):100–112.
- Burnside ES, Drukker K, Li H, et al. Using computer-extracted image phenotypes from tumors on breast magnetic resonance imaging to predict breast cancer pathologic stage. *Cancer* 2016;122(5):748–757.
- Li H, Zhu Y, Burnside ES, et al. MR imaging radiomics signatures for predicting the risk of breast cancer recurrence as given by research versions of MammaPrint, Oncotype DX, and PAM50 gene assays. *Radiology* 2016;281(2):382–391.
- Ashraf AB, Daye D, Gavenonis S, et al. Identification of intrinsic imaging phenotypes for breast cancer tumors: preliminary associations with gene expression profiles. *Radiology* 2014;272(2):374–384.
- Kim JH, Ko ES, Lim Y, et al. Breast cancer heterogeneity: MR imaging texture analysis and survival outcomes. *Radiology* 2017;282(3):665–675.
- Chamming's F, Ueno Y, Ferré R, et al. Features from computerized texture analysis of breast cancers at pretreatment MR imaging are associated with response to neoadjuvant chemotherapy. *Radiology* 2018;286(2):412–420.
- Gatenby RA, Grove O, Gillies RJ. Quantitative imaging in cancer evolution and ecology. *Radiology* 2013;269(1):8–15.
- Hylton N. Dynamic contrast-enhanced magnetic resonance imaging as an imaging biomarker. *J Clin Oncol* 2006;24(20):3293–3298.
- Yankeelov TE, Gore JC. Dynamic contrast enhanced magnetic resonance imaging in oncology: theory, data acquisition, analysis, and examples. *Curr Med Imaging Rev* 2009;3(2):91–107.
- Kapp AV, Tibshirani R. Are clusters found in one dataset present in another dataset? *Biostatistics* 2007;8(1):9–31.
- Tusher VG, Tibshirani R, Chu G. Significance analysis of microarrays applied to the ionizing radiation response. *Proc Natl Acad Sci U S A* 2001;98(9):5116–5121.
- von Luxburg U. A tutorial on spectral clustering. *Stat Comput* 2007;17(4):395–416.
- Raghavan UN, Albert R, Kumara S. Near linear time algorithm to detect community structures in large-scale networks. *Phys Rev E Stat Nonlin Soft Matter Phys* 2007;76(3 Pt 2):036106.
- Gradishar WJ, Anderson BO, Balassanian R, et al. Invasive breast cancer version 1.2016. NCCN clinical practice guidelines in oncology. *J Natl Compr Canc Netw* 2016;14(3):324–354.
- Davall F, Yip CS, Ljungqvist G, et al. Assessment of tumor heterogeneity: an emerging imaging tool for clinical practice? *Insights Imaging* 2012;3(6):573–589.
- O'Connor JP, Rose CJ, Waterton JC, Carano RA, Parker GJ, Jackson A. Imaging intratumor heterogeneity: role in therapy response, resistance, and clinical outcome. *Clin Cancer Res* 2015;21(2):249–257.
- Hylton NM, Blume JD, Bernreuter WK, et al. Locally advanced breast cancer: MR imaging for prediction of response to neoadjuvant chemotherapy—results from ACRIN 6657/I-SPY TRIAL. *Radiology* 2012;263(3):663–672.
- Yates LR, Gerstung M, Knappskog S, et al. Subclonal diversification of primary breast cancer revealed by multiregion sequencing. *Nat Med* 2015;21(7):751–759.
- Gerlinger M, Rowan AJ, Horswell S, et al. Intratumor heterogeneity and branched evolution revealed by multiregion sequencing. *N Engl J Med* 2012;366(10):883–892.
- Zhou M, Hall L, Goldgof D, et al. Radiologically defined ecological dynamics and clinical outcomes in glioblastoma multiforme: preliminary results. *Transl Oncol* 2014;7(1):5–13.
- Zhou M, Chaudhury B, Hall LO, Goldgof DB, Gillies RJ, Gatenby RA. Identifying spatial imaging biomarkers of glioblastoma multiforme for survival group prediction. *J Magn Reson Imaging* 2017;46(1):115–123.
- Cui Y, Tha KK, Terasaka S, et al. Prognostic imaging biomarkers in glioblastoma: development and independent validation on the basis of multiregion and quantitative analysis of MR images. *Radiology* 2016;278(2):546–553.
- Chaudhury B, Zhou M, Goldgof DB, et al. Heterogeneity in intratumoral regions with rapid gadolinium washout correlates with estrogen receptor status and nodal metastasis. *J Magn Reson Imaging* 2015;42(5):1421–1430.
- Wu J, Gong G, Cui Y, Li R. Intratumor partitioning and texture analysis of dynamic contrast-enhanced (DCE)-MRI identifies relevant tumor subregions to predict pathological response of breast cancer to neoadjuvant chemotherapy. *J Magn Reson Imaging* 2016;44(5):1107–1115.
- Semenza GL. The hypoxic tumor microenvironment: a driving force for breast cancer progression. *Biochim Biophys Acta* 2016;1863(3):382–391.
- Rankin EB, Giaccia AJ. Hypoxic control of metastasis. *Science* 2016;352(6282):175–180.
- Gilkes DM, Semenza GL. Role of hypoxia-inducible factors in breast cancer metastasis. *Future Oncol* 2013;9(11):1623–1636.
- Mankoff DA, Farwell MD, Clark AS, Pryma DA. Making molecular imaging a clinical tool for precision oncology: a review. *JAMA Oncol* 2017;3(5):695–701.
- Yankeelov TE, Mankoff DA, Schwartz LH, et al. Quantitative imaging in cancer clinical trials. *Clin Cancer Res* 2016;22(2):284–290.
- Fowler AM, Mankoff DA, Joe BN. Imaging neoadjuvant therapy response in breast cancer. *Radiology* 2017;285(2):358–375.
- Braman NM, Etesami M, Prasanna P, et al. Intratumoral and peritumoral radiomics for the pretreatment prediction of pathological complete response to neoadjuvant chemotherapy based on breast DCE-MRI. *Breast Cancer Res* 2017;19(1):57 [Published correction appears in *Breast Cancer Res* 2017;19(1):80].
- Bae MS, Shin SU, Ryu HS, et al. Pretreatment MR imaging features of triple-negative breast cancer: association with response to neoadjuvant chemotherapy and recurrence-free survival. *Radiology* 2016;281(2):392–400.
- Fukada I, Araki K, Kobayashi K, et al. Pattern of tumor shrinkage during neoadjuvant chemotherapy is associated with prognosis in low-grade luminal early breast cancer. *Radiology* 2018;286(1):49–57.
- Wu J, Li B, Sun X, et al. Heterogeneous enhancement patterns of tumor-adjacent parenchyma at MR imaging are associated with dysregulated signaling pathways and poor survival in breast cancer. *Radiology* 2017;285(2):401–413.
- Wu J, Cui Y, Sun X, et al. Unsupervised clustering of quantitative image phenotypes reveals breast cancer subtypes with distinct prognoses and molecular pathways. *Clin Cancer Res* 2017;23(13):3334–3342.